BABAR-CONF-03/019
SLAC-PUB-10100
hep-ex/0308016
August 2003

Measurement of the $B \to X_s\, \ell^+\ell^-$ Branching Fraction Using a Sum over Exclusive Modes

The *BABAR* Collaboration

August 7, 2003

Abstract

We present a measurement of the branching fraction for the flavor-changing neutral current process $B \to X_s\, \ell^+\ell^-$ based on a sample of 88.9×10^6 $\Upsilon(4S) \to B\overline{B}$ events recorded with the *BABAR* detector at the PEP-II e^+e^- storage ring. The final state is reconstructed from pairs of electrons or muons and a hadronic system consisting of one $K^\pm$ or K_s^0 and up to two pions, with at most one π^0. Summing over both lepton flavors, we observe a signal of $41 \pm 10(stat) \pm 2(syst)$ events with a statistical significance of $4.6\,\sigma$. The inclusive branching fraction is determined to be $\mathcal{B}(B \to X_s\, \ell^+\ell^-) = \left(6.3 \pm 1.6(stat)^{+1.8}_{-1.5}(syst)\right) \times 10^{-6}$ for $m(\ell^+\ell^-) > 0.2$ GeV/c^2. All results are preliminary.

Contributed to the XXIst International Symposium on Lepton and Photon Interactions at High Energies, 8/11 — 8/16/2003, Fermilab, Illinois, USA.

Stanford Linear Accelerator Center, Stanford University, Stanford, CA 94309

Work supported in part by Department of Energy contract DE-AC03-76SF00515.

The *BABAR* Collaboration,

B. Aubert, R. Barate, D. Boutigny, J.-M. Gaillard, A. Hicheur, Y. Karyotakis, J. P. Lees, P. Robbe, V. Tisserand, A. Zghiche

Laboratoire de Physique des Particules, F-74941 Annecy-le-Vieux, France

A. Palano, A. Pompili

Università di Bari, Dipartimento di Fisica and INFN, I-70126 Bari, Italy

J. C. Chen, N. D. Qi, G. Rong, P. Wang, Y. S. Zhu

Institute of High Energy Physics, Beijing 100039, China

G. Eigen, I. Ofte, B. Stugu

University of Bergen, Inst. of Physics, N-5007 Bergen, Norway

G. S. Abrams, A. W. Borgland, A. B. Breon, D. N. Brown, J. Button-Shafer, R. N. Cahn, E. Charles, C. T. Day, M. S. Gill, A. V. Gritsan, Y. Groysman, R. G. Jacobsen, R. W. Kadel, J. Kadyk, L. T. Kerth, Yu. G. Kolomensky, J. F. Kral, G. Kukartsev, C. LeClerc, M. E. Levi, G. Lynch, L. M. Mir, P. J. Oddone, T. J. Orimoto, M. Pripstein, N. A. Roe, A. Romosan, M. T. Ronan, V. G. Shelkov, A. V. Telnov, W. A. Wenzel

Lawrence Berkeley National Laboratory and University of California, Berkeley, CA 94720, USA

K. Ford, T. J. Harrison, C. M. Hawkes, D. J. Knowles, S. E. Morgan, R. C. Penny, A. T. Watson, N. K. Watson

University of Birmingham, Birmingham, B15 2TT, United Kingdom

T. Held, K. Goetzen, H. Koch, B. Lewandowski, M. Pelizaeus, K. Peters, H. Schmuecker, M. Steinke

Ruhr Universität Bochum, Institut für Experimentalphysik 1, D-44780 Bochum, Germany

N. R. Barlow, J. T. Boyd, N. Chevalier, W. N. Cottingham, M. P. Kelly, T. E. Latham, C. Mackay, F. F. Wilson

University of Bristol, Bristol BS8 1TL, United Kingdom

K. Abe, T. Cuhadar-Donszelmann, C. Hearty, T. S. Mattison, J. A. McKenna, D. Thiessen

University of British Columbia, Vancouver, BC, Canada V6T 1Z1

P. Kyberd, A. K. McKemey

Brunel University, Uxbridge, Middlesex UB8 3PH, United Kingdom

V. E. Blinov, A. D. Bukin, V. B. Golubev, V. N. Ivanchenko, E. A. Kravchenko, A. P. Onuchin, S. I. Serednyakov, Yu. I. Skovpen, E. P. Solodov, A. N. Yushkov

Budker Institute of Nuclear Physics, Novosibirsk 630090, Russia

D. Best, M. Bruinsma, M. Chao, D. Kirkby, A. J. Lankford, M. Mandelkern, R. K. Mommsen, W. Roethel, D. P. Stoker

University of California at Irvine, Irvine, CA 92697, USA

C. Buchanan, B. L. Hartfiel

University of California at Los Angeles, Los Angeles, CA 90024, USA

B. C. Shen

University of California at Riverside, Riverside, CA 92521, USA

D. del Re, H. K. Hadavand, E. J. Hill, D. B. MacFarlane, H. P. Paar, Sh. Rahatlou, V. Sharma

University of California at San Diego, La Jolla, CA 92093, USA

J. W. Berryhill, C. Campagnari, B. Dahmes, N. Kuznetsova, S. L. Levy, O. Long, A. Lu, M. A. Mazur, J. D. Richman, W. Verkerke

University of California at Santa Barbara, Santa Barbara, CA 93106, USA

T. W. Beck, J. Beringer, A. M. Eisner, C. A. Heusch, W. S. Lockman, T. Schalk, R. E. Schmitz, B. A. Schumm, A. Seiden, M. Turri, W. Walkowiak, D. C. Williams, M. G. Wilson

University of California at Santa Cruz, Institute for Particle Physics, Santa Cruz, CA 95064, USA

J. Albert, E. Chen, G. P. Dubois-Felsmann, A. Dvoretskii, D. G. Hitlin, I. Narsky, F. C. Porter, A. Ryd, A. Samuel, S. Yang

California Institute of Technology, Pasadena, CA 91125, USA

S. Jayatilleke, G. Mancinelli, B. T. Meadows, M. D. Sokoloff

University of Cincinnati, Cincinnati, OH 45221, USA

T. Abe, F. Blanc, P. Bloom, S. Chen, P. J. Clark, W. T. Ford, U. Nauenberg, A. Olivas, P. Rankin, J. Roy, J. G. Smith, W. C. van Hoek, L. Zhang

University of Colorado, Boulder, CO 80309, USA

J. L. Harton, T. Hu, A. Soffer, W. H. Toki, R. J. Wilson, J. Zhang

Colorado State University, Fort Collins, CO 80523, USA

D. Altenburg, T. Brandt, J. Brose, T. Colberg, M. Dickopp, R. S. Dubitzky, A. Hauke, H. M. Lacker, E. Maly, R. Müller-Pfefferkorn, R. Nogowski, S. Otto, J. Schubert, K. R. Schubert, R. Schwierz, B. Spaan, L. Wilden

Technische Universität Dresden, Institut für Kern- und Teilchenphysik, D-01062 Dresden, Germany

D. Bernard, G. R. Bonneaud, F. Brochard, J. Cohen-Tanugi, P. Grenier, Ch. Thiebaux, G. Vasileiadis, M. Verderi

Ecole Polytechnique, LLR, F-91128 Palaiseau, France

A. Khan, D. Lavin, F. Muheim, S. Playfer, J. E. Swain

University of Edinburgh, Edinburgh EH9 3JZ, United Kingdom

M. Andreotti, V. Azzolini, D. Bettoni, C. Bozzi, R. Calabrese, G. Cibinetto, E. Luppi, M. Negrini, L. Piemontese, A. Sarti

Università di Ferrara, Dipartimento di Fisica and INFN, I-44100 Ferrara, Italy

E. Treadwell

Florida A&M University, Tallahassee, FL 32307, USA

F. Anulli,[1] R. Baldini-Ferroli, M. Biasini,[1] A. Calcaterra, R. de Sangro, D. Falciai, G. Finocchiaro, P. Patteri, I. M. Peruzzi,[1] M. Piccolo, M. Pioppi,[1] A. Zallo

Laboratori Nazionali di Frascati dell'INFN, I-00044 Frascati, Italy

[1]Also with Università di Perugia, Perugia, Italy

A. Buzzo, R. Capra, R. Contri, G. Crosetti, M. Lo Vetere, M. Macri, M. R. Monge, S. Passaggio, C. Patrignani, E. Robutti, A. Santroni, S. Tosi

Università di Genova, Dipartimento di Fisica and INFN, I-16146 Genova, Italy

S. Bailey, M. Morii, E. Won

Harvard University, Cambridge, MA 02138, USA

W. Bhimji, D. A. Bowerman, P. D. Dauncey, U. Egede, I. Eschrich, J. R. Gaillard, G. W. Morton, J. A. Nash, P. Sanders, G. P. Taylor

Imperial College London, London, SW7 2BW, United Kingdom

G. J. Grenier, S.-J. Lee, U. Mallik

University of Iowa, Iowa City, IA 52242, USA

J. Cochran, H. B. Crawley, J. Lamsa, W. T. Meyer, S. Prell, E. I. Rosenberg, J. Yi

Iowa State University, Ames, IA 50011-3160, USA

M. Davier, G. Grosdidier, A. Höcker, S. Laplace, F. Le Diberder, V. Lepeltier, A. M. Lutz, T. C. Petersen, S. Plaszczynski, M. H. Schune, L. Tantot, G. Wormser

Laboratoire de l'Accélérateur Linéaire, F-91898 Orsay, France

V. Brigljević , C. H. Cheng, D. J. Lange, D. M. Wright

Lawrence Livermore National Laboratory, Livermore, CA 94550, USA

A. J. Bevan, J. P. Coleman, J. R. Fry, E. Gabathuler, R. Gamet, M. Kay, R. J. Parry, D. J. Payne, R. J. Sloane, C. Touramanis

University of Liverpool, Liverpool L69 3BX, United Kingdom

J. J. Back, P. F. Harrison, H. W. Shorthouse, P. Strother, P. B. Vidal

Queen Mary, University of London, E1 4NS, United Kingdom

C. L. Brown, G. Cowan, R. L. Flack, H. U. Flaecher, S. George, M. G. Green, A. Kurup, C. E. Marker, T. R. McMahon, S. Ricciardi, F. Salvatore, G. Vaitsas, M. A. Winter

University of London, Royal Holloway and Bedford New College, Egham, Surrey TW20 0EX, United Kingdom

D. Brown, C. L. Davis

University of Louisville, Louisville, KY 40292, USA

J. Allison, R. J. Barlow, A. C. Forti, P. A. Hart, M. C. Hodgkinson, F. Jackson, G. D. Lafferty, A. J. Lyon, J. H. Weatherall, J. C. Williams

University of Manchester, Manchester M13 9PL, United Kingdom

A. Farbin, A. Jawahery, D. Kovalskyi, C. K. Lae, V. Lillard, D. A. Roberts

University of Maryland, College Park, MD 20742, USA

G. Blaylock, C. Dallapiccola, K. T. Flood, S. S. Hertzbach, R. Kofler, V. B. Koptchev, T. B. Moore, S. Saremi, H. Staengle, S. Willocq

University of Massachusetts, Amherst, MA 01003, USA

R. Cowan, G. Sciolla, F. Taylor, R. K. Yamamoto

Massachusetts Institute of Technology, Laboratory for Nuclear Science, Cambridge, MA 02139, USA

D. J. J. Mangeol, P. M. Patel

McGill University, Montréal, QC, Canada H3A 2T8

A. Lazzaro, F. Palombo

Università di Milano, Dipartimento di Fisica and INFN, I-20133 Milano, Italy

J. M. Bauer, L. Cremaldi, V. Eschenburg, R. Godang, R. Kroeger, J. Reidy, D. A. Sanders, D. J. Summers, H. W. Zhao

University of Mississippi, University, MS 38677, USA

S. Brunet, D. Cote-Ahern, C. Hast, P. Taras

Université de Montréal, Laboratoire René J. A. Lévesque, Montréal, QC, Canada H3C 3J7

H. Nicholson

Mount Holyoke College, South Hadley, MA 01075, USA

C. Cartaro, N. Cavallo,[2] G. De Nardo, F. Fabozzi,[2] C. Gatto, L. Lista, P. Paolucci, D. Piccolo, C. Sciacca

Università di Napoli Federico II, Dipartimento di Scienze Fisiche and INFN, I-80126, Napoli, Italy

M. A. Baak, G. Raven

NIKHEF, National Institute for Nuclear Physics and High Energy Physics, NL-1009 DB Amsterdam, The Netherlands

J. M. LoSecco

University of Notre Dame, Notre Dame, IN 46556, USA

T. A. Gabriel

Oak Ridge National Laboratory, Oak Ridge, TN 37831, USA

B. Brau, K. K. Gan, K. Honscheid, D. Hufnagel, H. Kagan, R. Kass, T. Pulliam, Q. K. Wong

Ohio State University, Columbus, OH 43210, USA

J. Brau, R. Frey, C. T. Potter, N. B. Sinev, D. Strom, E. Torrence

University of Oregon, Eugene, OR 97403, USA

F. Colecchia, A. Dorigo, F. Galeazzi, M. Margoni, M. Morandin, M. Posocco, M. Rotondo, F. Simonetto, R. Stroili, G. Tiozzo, C. Voci

Università di Padova, Dipartimento di Fisica and INFN, I-35131 Padova, Italy

M. Benayoun, H. Briand, J. Chauveau, P. David, Ch. de la Vaissière, L. Del Buono, O. Hamon, M. J. J. John, Ph. Leruste, J. Ocariz, M. Pivk, L. Roos, J. Stark, S. T'Jampens, G. Therin

Universités Paris VI et VII, Lab de Physique Nucléaire H. E., F-75252 Paris, France

P. F. Manfredi, V. Re

Università di Pavia, Dipartimento di Elettronica and INFN, I-27100 Pavia, Italy

[2]Also with Università della Basilicata, Potenza, Italy

P. K. Behera, L. Gladney, Q. H. Guo, J. Panetta

University of Pennsylvania, Philadelphia, PA 19104, USA

C. Angelini, G. Batignani, S. Bettarini, M. Bondioli, F. Bucci, G. Calderini, M. Carpinelli, V. Del Gamba, F. Forti, M. A. Giorgi, A. Lusiani, G. Marchiori, F. Martinez-Vidal,[3] M. Morganti, N. Neri, E. Paoloni, M. Rama, G. Rizzo, F. Sandrelli, J. Walsh

Università di Pisa, Dipartimento di Fisica, Scuola Normale Superiore and INFN, I-56127 Pisa, Italy

M. Haire, D. Judd, K. Paick, D. E. Wagoner

Prairie View A&M University, Prairie View, TX 77446, USA

N. Danielson, P. Elmer, C. Lu, V. Miftakov, J. Olsen, A. J. S. Smith, H. A. Tanaka E. W. Varnes

Princeton University, Princeton, NJ 08544, USA

F. Bellini, G. Cavoto,[4] R. Faccini,[5] F. Ferrarotto, F. Ferroni, M. Gaspero, M. A. Mazzoni, S. Morganti, M. Pierini, G. Piredda, F. Safai Tehrani, C. Voena

Università di Roma La Sapienza, Dipartimento di Fisica and INFN, I-00185 Roma, Italy

S. Christ, G. Wagner, R. Waldi

Universität Rostock, D-18051 Rostock, Germany

T. Adye, N. De Groot, B. Franek, N. I. Geddes, G. P. Gopal, E. O. Olaiya, S. M. Xella

Rutherford Appleton Laboratory, Chilton, Didcot, Oxon, OX11 0QX, United Kingdom

R. Aleksan, S. Emery, A. Gaidot, S. F. Ganzhur, P.-F. Giraud, G. Hamel de Monchenault, W. Kozanecki, M. Langer, M. Legendre, G. W. London, B. Mayer, G. Schott, G. Vasseur, Ch. Yeche, M. Zito

DSM/Dapnia, CEA/Saclay, F-91191 Gif-sur-Yvette, France

M. V. Purohit, A. W. Weidemann, F. X. Yumiceva

University of South Carolina, Columbia, SC 29208, USA

D. Aston, R. Bartoldus, N. Berger, A. M. Boyarski, O. L. Buchmueller, M. R. Convery, D. P. Coupal, D. Dong, J. Dorfan, D. Dujmic, W. Dunwoodie, R. C. Field, T. Glanzman, S. J. Gowdy, E. Grauges-Pous, T. Hadig, V. Halyo, T. Hryn'ova, W. R. Innes, C. P. Jessop, M. H. Kelsey, P. Kim, M. L. Kocian, U. Langenegger, D. W. G. S. Leith, S. Luitz, V. Luth, H. L. Lynch, H. Marsiske, R. Messner, D. R. Muller, C. P. O'Grady, V. E. Ozcan, A. Perazzo, M. Perl, S. Petrak, B. N. Ratcliff, S. H. Robertson, A. Roodman, A. A. Salnikov, R. H. Schindler, J. Schwiening, G. Simi, A. Snyder, A. Soha, J. Stelzer, D. Su, M. K. Sullivan, J. Va'vra, S. R. Wagner, M. Weaver, A. J. R. Weinstein, W. J. Wisniewski, D. H. Wright, C. C. Young

Stanford Linear Accelerator Center, Stanford, CA 94309, USA

P. R. Burchat, A. J. Edwards, T. I. Meyer, B. A. Petersen, C. Roat

Stanford University, Stanford, CA 94305-4060, USA

S. Ahmed, M. S. Alam, J. A. Ernst, M. Saleem, F. R. Wappler

State Univ. of New York, Albany, NY 12222, USA

[3]Also with IFIC, Instituto de Física Corpuscular, CSIC-Universidad de Valencia, Valencia, Spain

[4]Also with Princeton University

[5]Also with University of California at San Diego

W. Bugg, M. Krishnamurthy, S. M. Spanier
University of Tennessee, Knoxville, TN 37996, USA

R. Eckmann, H. Kim, J. L. Ritchie, R. F. Schwitters
University of Texas at Austin, Austin, TX 78712, USA

J. M. Izen, I. Kitayama, X. C. Lou, S. Ye
University of Texas at Dallas, Richardson, TX 75083, USA

F. Bianchi, M. Bona, F. Gallo, D. Gamba
Università di Torino, Dipartimento di Fisica Sperimentale and INFN, I-10125 Torino, Italy

C. Borean, L. Bosisio, G. Della Ricca, S. Dittongo, S. Grancagnolo, L. Lanceri, P. Poropat,[6] L. Vitale, G. Vuagnin
Università di Trieste, Dipartimento di Fisica and INFN, I-34127 Trieste, Italy

R. S. Panvini
Vanderbilt University, Nashville, TN 37235, USA

Sw. Banerjee, C. M. Brown, D. Fortin, P. D. Jackson, R. Kowalewski, J. M. Roney
University of Victoria, Victoria, BC, Canada V8W 3P6

H. R. Band, S. Dasu, M. Datta, A. M. Eichenbaum, J. R. Johnson, P. E. Kutter, H. Li, R. Liu, F. Di Lodovico, A. Mihalyi, A. K. Mohapatra, Y. Pan, R. Prepost, S. J. Sekula, J. H. von Wimmersperg-Toeller, J. Wu, S. L. Wu, Z. Yu
University of Wisconsin, Madison, WI 53706, USA

H. Neal
Yale University, New Haven, CT 06511, USA

[6]Deceased

1 Introduction

The rare decay $B \to X_s\, \ell^+\ell^-$ proceeds through a $b \to s\ell^+\ell^-$ transition, which is forbidden at tree level in the Standard Model (SM). However, such a flavor-changing neutral current (FCNC) process can occur at higher order via electroweak penguin and W^+W^- box diagrams, as shown in Figure 1. The $b \to s\ell^+\ell^-$ transition therefore allows deeper insight into the effective Hamiltonian describing FCNC processes and is sensitive to the effects of non-SM physics that may enter these loops; see, for example, Refs. [1, 2].

Recent calculations of the branching fractions for the exclusive decay modes predict $\mathcal{B}(B \to Ke^+e^-) = \mathcal{B}(B \to K\mu^+\mu^-) = (0.35 \pm 0.12) \times 10^{-6}$, $\mathcal{B}(B \to K^*e^+e^-) = (1.58 \pm 0.49) \times 10^{-6}$ and $\mathcal{B}(B \to K^*\mu^+\mu^-) = (1.19 \pm 0.39) \times 10^{-6}$, and for the inclusive processes $\mathcal{B}(B \to X_s\, e^+e^-) = (6.9 \pm 1.0) \times 10^{-6}$ and $\mathcal{B}(B \to X_s\mu^+\mu^-) = (4.2 \pm 0.7) \times 10^{-6}$ [1]. In the electron channel, the branching fraction is predicted to be $\mathcal{B}(B \to X_s\, e^+e^-) = (4.2 \pm 0.7) \times 10^{-6}$ [3] for $m(e^+e^-) > 0.2$ GeV/c^2. Measurements of the inclusive branching fractions are motivated by the smaller theoretical uncertainties, as compared with predictions for exclusive decays. Both the Belle and *BABAR* Collaborations have observed the $B \to K\ell^+\ell^-$ ($\ell = e, \mu$) decay [4, 5], *BABAR* has found evidence for the $B \to K^*\ell^+\ell^-$ decay [6], and Belle has measured the inclusive $B \to X_s\, \ell^+\ell^-$ decay [7].

In the present analysis, we study the $B \to X_s\ell^+\ell^-$ process by reconstructing the final state from pairs of electrons or muons and a hadronic system consisting of one $K^\pm$ or K^0_s and up to two pions, with at most one π^0. The choice of maximum number of pions is motivated by the fact that the signal-to-background ratio drops significantly with increasing multiplicity. This approach [8], which sums over exclusive modes, allows approximately half of the full inclusive rate to be reconstructed. If the fraction of modes containing a K^0_L is taken to be equal to that containing a K^0_S, the missing states that remain unaccounted for represent ∼25% of the total rate. We require the hadronic mass for the selected final states to be less than 1.8 GeV/c^2 to reduce combinatorial background. This cut retains approximately 94% of the signal in the reconstructed modes. We correct for the missing modes and the effect of the hadronic mass cut to extract the inclusive $B \to X_s\, \ell^+\ell^-$ decay rate for $m(\ell^+\ell^-) > 0.2$ GeV/c^2.

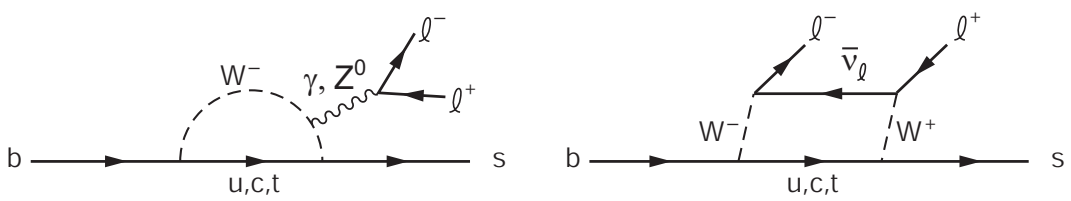

Figure 1: Feynman diagrams for $b \to s\ell^+\ell^-$ transitions.

2 The *BABAR* Detector and Data Sample

The data sample used in this analysis was collected with the *BABAR* detector during 1999-2002 at the PEP-II asymmetric-energy e^+e^- storage ring at the Stanford Linear Accelerator Center. It consists of 81.9 fb^{-1} recorded at the $\Upsilon(4S)$ resonance, corresponding to 88.9×10^6 $\Upsilon(4S) \to B\overline{B}$ events, as well as an additional 9.6 fb^{-1} recorded 40 MeV below the $\Upsilon(4S)$ resonance. The off-resonance data provide a clean sample of $e^+e^- \to q\bar{q}$ (with $q = u, d, s, c$) continuum events for

background studies.

This analysis relies on the charged-particle tracking systems and particle identification systems of the *BABAR* detector [9]. A 5-layer silicon vertex tracker (SVT) and a 40-layer drift chamber (DCH) provide tracking and particle identification for charged particles. The DIRC, a Cherenkov ring-imaging system, is primarily used for charged hadron (π, K, p) identification. The electromagnetic calorimeter (EMC), consisting of Tl-doped CsI crystals, provides electron identification and photon reconstruction. These detectors are located inside a 1.5-T solenoidal superconducting magnet. Muons are identified in the instrumented flux return (IFR) with resistive plate chambers interleaved with iron plates.

Clean particle identification for the final state particles $e^{\pm}$, $\mu^{\pm}$, $K^{\pm}$, K^0_s, $\pi^{\pm}$ and π^0 is important for this analysis. Electrons and muons are required to have lab-frame momenta greater than 0.5 GeV/c and 1.0 GeV/c, respectively. Bremsstrahlung photons from electrons are recovered by combining an electron with up to three photons within a small angular region around the electron direction [10]. K^0_s candidates are reconstructed from pairs of oppositely-charged tracks with $|m(\pi^+\pi^-) - m(K^0_s)| < 11.2$ MeV/c^2, decay length greater than 2 mm, and angle between the K^0_s momentum vector and the line between the primary vertex and the K^0_s vertex satisfying $\cos\delta > 0.99$. Charged pions are selected from tracks after rejection of cleanly identified $e^{\pm}$ and $K^{\pm}$ candidates. Neutral pions are required to have lab-frame energy greater than 400 MeV, photon daughter energies greater than 50 MeV, and a $\gamma\gamma$ invariant mass that satisfies $|m(\gamma\gamma) - m(\pi^0)| < 10$ MeV/c^2.

3 Analysis overview

We use a technique that sums over exclusive modes to measure the inclusive branching fraction $\mathcal{B}(B \to X_s\, \ell^+\ell^-)$. Compared to a fully inclusive approach, this method has the advantage of being able to exploit the strong kinematical discrimination provided by $m_{ES} = \sqrt{E^2_{beam} - \vec{p}^{\,2}_B}$ and $\Delta E = E_B - E_{beam}$, where E_{beam} is the beam energy and E_B ($\vec{p}_B$) is the reconstructed B meson energy (3-momentum). All quantities are evaluated in the e^+e^- center-of-mass system (CM). This analysis approach is needed to suppress large backgrounds from $B\overline{B}$ and continuum events, and to extract the expected small signal yield.

The main contribution to the combinatorial background is from semileptonic decays in $B\overline{B}$ events. In these events, $B \to X_s\, \ell^+\ell^-$ candidates contain decay products from both B mesons (i.e., the daughters of the $B \to X_s\, \ell^+\ell^-$ candidate do not originate from the same point) and there is a significant amount of missing energy due to neutrinos. Another contribution to the combinatorial background is due to continuum events, which are effectively suppressed with event-shape variables.

The dominant peaking backgrounds, which are from $B \to J/\psi X$ and $B \to \psi(2S)X$ decays with $J/\psi(\psi(2S)) \to \ell^+\ell^-$, mimic the signal and need to be efficiently removed with cuts on the dilepton mass $m(\ell^+\ell^-)$. The resulting veto sample provides a large control sample of decays with a signature identical to that of the signal, albeit in a restricted range of $m(\ell^+\ell^-)$. $B \to D^{(*)}n\pi$ $(n > 0)$ decays with misidentification of two charged pions as leptons present an additional source of peaking background.

Simulated $B \to X_s\, \ell^+\ell^-$ events are produced with a combination of exclusive and inclusive models. In the hadronic mass region of $m(X_s) < 1.1$ GeV/c^2, exclusive $B \to K^{(*)}\ell^+\ell^-$ decays are generated according to [1, 11], where the relevant form factors are computed using light-cone QCD sum rules. The remaining decays, in the region $m(X_s) > 1.1$ GeV/c^2, are generated with

a nonresonant model following [1, 12] and using the Fermi motion model of [13]. JETSET [14] is then used to hadronize the system consisting of a strange quark and a spectator quark.

4 Event selection

Events are required to have a well determined primary vertex, be tagged as multi-hadron events, have a ratio of the second to zeroth-order Fox-Wolfram moments [15] (calculated using charged tracks and neutral calorimeter clusters) of $R_2 < 0.5$, have at least four charged tracks, and contain at least two leptons (either electrons or muons) satisfying loose particle identification criteria and having lab-frame momenta greater than 0.5 GeV/c for electrons and 0.8 GeV/c for muons.

In the next step, B candidates are reconstructed. A dilepton is selected by choosing the e^+e^- or $\mu^+\mu^-$ pair with the largest value of $|p(\ell^+)| + |p(\ell^-)|$, using lab-frame momenta. The dilepton candidate is required to form a good vertex. Using this $\ell^+\ell^-$ pair, $B \to X_s\ell^+\ell^-$ candidates are formed by adding either a $K^\pm$ or a K_s^0 and up to two pions, but no more than one π^0. In this manner, ten different hadronic topologies are considered: K^+, $K^+\pi^0$, $K^+\pi^-$, $K^+\pi^-\pi^0$, $K^+\pi^-\pi^+$, K_S^0, $K_S^0\pi^0$, $K_S^0\pi^+$, $K_S^0\pi^+\pi^0$, and $K_S^0\pi^+\pi^-$.

The resulting B candidates are required to have an $\ell^+\ell^-$ vertex fit probability $\log(P_{llvtx}) > -10$, a B vertex constructed from charged daughter particles with fit probability $\log(P_{Bvtx}) > -10$, $m(X_s) < 2.5$ GeV/c^2, $5.0 < m_{ES} < 5.29$ GeV/c^2, and $|\Delta E| < 0.3$ GeV.

At this stage, there is an average of five B candidates per event in the signal simulation. Only the B candidate with the largest signal likelihood value is retained. The signal likelihood function is constructed based on the simulated distributions of ΔE, $\log(P_{Bvtx})$, and $\cos\theta_B$ for the signal, where θ_B is the angle between the momentum vector of the B candidate and the beam axis in the CM frame. We select the best candidate before further selection cuts are applied. This approach entails a small cost in signal efficiency, which is more than compensated by an improved background suppression in the final sample.

After selecting the best candidate, combinatorial backgrounds are suppressed by tightening some of the earlier requirements: $m(X_s) < 1.8$ GeV/c^2, $5.20 < m_{ES} < 5.29$ GeV/c^2, and $-0.2 < \Delta E < 0.1$ GeV. In addition, we require the separation between the two leptons along the beam direction to satisfy $|\Delta z| < 0.15$ cm, where the z-coordinate of each lepton is determined at the point of closest approach to the beam axis. We also require the rest of the event, formed by combining all charged tracks and neutral calorimeter clusters not included in the B candidate, to satisfy $-5.0 < \Delta E^{ROE} < 2.0$ GeV and $m_{ES}^{ROE} > 4.9$ GeV/c^2.

Charmonium backgrounds are reduced by removing B candidates with dilepton mass in the ranges $2.70 < m(e^+e^-) < 3.25$ GeV/c^2, $2.80 < m(\mu^+\mu^-) < 3.20$ GeV/c^2, $3.45 < m(e^+e^-) < 3.80$ GeV/c^2, and $3.55 < m(\mu^+\mu^-) < 3.80$ GeV/c^2. If one of the electrons from a J/ψ or $\psi(2S)$ decay erroneously picks up a random photon in the Bremsstrahlung-recovery process, the dilepton mass can increase sufficiently to evade the above cuts. Therefore the charmonium veto is applied to the dilepton mass before and after Bremsstrahlung recovery. Using the simulation, we estimate the remaining peaking charmonium background to be 0.6 ± 0.3 events and 0.3 ± 0.2 events for e^+e^- modes and $\mu^+\mu^-$ modes, respectively.

The potential peaking background from $B \to X_s\gamma$ decays, followed by conversion of the photon into an e^+e^- pair in the detector material, is a concern for the e^+e^- modes only. After observing an excess of events in data over the simulation for low e^+e^- mass in the $m_{ES} < 5.27$ GeV/c^2 sideband distribution, we completely remove this background by requiring $m(e^+e^-) > 0.2$ GeV/c^2.

The final suppression of the combinatorial background is achieved with a likelihood ratio $\mathcal{L}_R$

based on nine variables: ΔE, ΔE^{ROE}, m_{ES}^{ROE}, Δz, $\log(P_{Bvtx})$, $\cos\theta_{miss}$, where θ_{miss} is the angle between the missing momentum vector for the whole event and the z axis in the CM frame, $\cos\theta_B$, $|\cos\theta_T|$, where θ_T is the angle between the thrust axes of the B candidate and the rest of the event in the CM frame, and R_2. The variables ΔE, ΔE^{ROE}, and m_{ES}^{ROE} are most effective at rejecting $B\overline{B}$ background, especially for events with two semileptonic decays, which have large missing energy. For continuum suppression, the event-shape variables $|\cos\theta_T|$ and R_2 are most useful. The distribution for the background-discrimination variable i is parameterized by a PDF η_i^j for each component j of the sample: $j = 1$ for signal, $j = 2$ for $B\overline{B}$ background, and $j = 3$ for continuum background. A likelihood is then computed for each sample component as the product of the individual PDFs for that component: $\mathcal{L}^j = \prod_i \eta_i^j$. The ratio between the likelihood for the signal component and the sum of the signal and background likelihoods then provides the final discriminating variable, the likelihood ratio $\mathcal{L}_R = \mathcal{L}^{signal}/(\mathcal{L}^{signal} + \mathcal{L}^{B\overline{B}} + \mathcal{L}^{cont})$.

Using the simulation, the cut on $\mathcal{L}_R$ is optimized to maximize the statistical significance of the signal. This optimization is performed separately for e^+e^- modes and $\mu^+\mu^-$ modes in the three $m(X_s)$ regions $m(X_s) < 0.6$ GeV/c^2, $0.6 < m(X_s) < 1.1$ GeV/c^2, and $1.1 < m(X_s) < 1.8$ GeV/c^2, resulting in the cuts $\mathcal{L}_R > 0.3$, 0.4, and 0.9 for the e^+e^- modes and $\mathcal{L}_R > 0.2$, 0.6, and 0.9 for the $\mu^+\mu^-$ modes.

After applying all selection criteria, a sample of 349 $B \to X_s\, e^+e^-$ and 222 $B \to X_s\, \mu^+\mu^-$ candidates remains. According to the simulation, the background left at this stage of the analysis consists mostly of $B\overline{B}$ events (86% and 72% of the total background in the electron and muon channels, respectively).

5 Maximum likelihood fit

We perform an extended, unbinned maximum likelihood fit to the m_{ES} distribution in the region $m_{ES} > 5.2$ GeV/c^2 to extract the signal yield as well as the shape and yield of the combinatorial background. The likelihood function $\mathcal{L}$ consists of four components:

$$\mathcal{L} = \frac{e^{-(N_{sig}+N_{c-peak}+N_{h-peak}+N_{comb})}}{N!} \prod_{k=1}^{N} [(N_{sig} + N_{c-peak})\mathcal{P}_k^{c-peak} + N_{h-peak}\mathcal{P}_k^{h-peak} + N_{comb}\mathcal{P}_k^{comb}] \tag{1}$$

where N and k denote the total number and index of candidate events, respectively. N_{sig}, N_{c-peak}, N_{h-peak}, and N_{comb} represent the yields of the signal, charmonium peaking background, hadronic peaking background, and combinatorial background, respectively, with corresponding PDFs given by $\mathcal{P}_k^{c-peak}$, $\mathcal{P}_k^{h-peak}$, and $\mathcal{P}_k^{comb}$. The signal PDF is the same as that for the charmonium peaking background since it is extracted from the charmonium-veto data sample.

The signal PDF $\mathcal{P}_k^{c-peak}$ is described by a Gaussian for $\mu^+\mu^-$ modes as well as for e^+e^- modes, since the Bremsstrahlung recovery and selection procedure for e^+e^- modes lead to a negligible radiative tail in the m_{ES} distribution. The Gaussian shape parameters are determined from fits to the sum of a Gaussian and Argus [16] function for the charmonium-veto data sample. The fits yield signal m_{ES} peak positions and resolutions of $m_{sig} = 5280.04 \pm 0.05$ MeV/c^2 and $\sigma_{sig} = 2.80 \pm 0.05$ MeV/c^2 for the e^+e^- modes, and $m_{sig} = 5280.05 \pm 0.07$ MeV/c^2 and $\sigma_{sig} = 2.61 \pm 0.06$ MeV/c^2 for the $\mu^+\mu^-$ modes, respectively. In the simulation, the Gaussian fit results for the m_{ES} distributions for correctly reconstructed signal are in agreement with the shape parameters extracted from the fits to the charmonium-veto sample. The signal yield N_{sig} is a free parameter in the likelihood fit.

The charmonium peaking background is estimated from the simulation to contribute $N_{c-peak} = 0.6 \pm 0.3$ events in the electron modes and $N_{c-peak} = 0.3 \pm 0.2$ events in the muon modes. In the likelihood fit, N_{c-peak} is fixed to these values.

The size and shape of the hadronic peaking $B\overline{B}$ background component arising from $B \to D^{(*)}n\pi$ $(n > 0)$ decays with misidentification of two charged pions as leptons are derived directly from data by performing the analysis without the lepton identification requirements. Parameters for the PDF $\mathcal{P}_k^{h-peak}$ are taken from a fit to the sum of a Gaussian and Argus function, with m_{ES} peak positions and resolutions of $m_{peak} = 5280.13 \pm 0.06$ MeV/c^2 and $\sigma_{peak} = 2.99 \pm 0.07$ MeV/c^2. Taking the π to ℓ misidentification rates into account, the remaining hadronic peaking backgrounds are estimated to be $N_{h-peak} = 2.4 \pm 0.8$ events for the $\mu^+\mu^-$ modes and are negligible for the e^+e^- modes. In the likelihood fit, N_{h-peak} is fixed to the estimated values.

The combinatorial background PDF, $\mathcal{P}_k^{comb}$, is given by an Argus shape, which describes the combinatorial contribution from continuum events and $B\overline{B}$ events. The Argus cutoff is determined by the beam energy in the $\Upsilon(4S)$ rest frame, $E_{beam} = 5.290$ GeV, whereas the Argus shape parameter and the yield N_{comb} are free parameters in the likelihood fit.

6 Results

Using the fit parameterizations described above, we fit the m_{ES} distributions for the selected $B \to X_s\, e^+e^-$ and $B \to X_s\, \mu^+\mu^-$ candidates separately and obtain the results shown in Figure 2. The fit results are summarized in Table 1. The statistical significance is $\mathcal{S} = \sqrt{2(\ln \mathcal{L}_{max} - \ln \mathcal{L}^0_{max})}$, where $\mathcal{L}_{max}$ represents the maximum likelihood for the fit and $\mathcal{L}^0_{max}$ denotes the maximum likelihood for a different fit when the signal yield is fixed at $N_{sig} = 0$. The significance does not incorporate effects due to systematic uncertainties in the signal shape or in the contribution from peaking background. However, these have been found to be small. The $B \to X_s\, \ell^+\ell^-$ signal yield presented in Table 1 is the sum of the $B \to X_s\, e^+e^-$ and $B \to X_s\, \mu^+\mu^-$ signal yields. A separate fit to the combined electron and muon channels gives a very similar result.

Figure 2(d) shows the distribution of m_{ES} for $B \to X_s\, e^\pm\mu^\mp$ candidates selected using the nominal selection criteria but requiring that the two leptons have different flavor. This sample provides a cross-check for the parameterization of the combinatorial background. Figure 2(d) shows an Argus fit to the m_{ES} distribution and, as expected, there is no evidence for peaking background. The Argus shape and yield parameters for the combinatorial background are free in the nominal fit to data.

Figure 3 shows the distribution of $m(X_s)$ for electron and muon channels combined. This distribution is obtained by performing the nominal likelihood fit in separate $m(X_s)$ regions. Figure 3 indicates that the observed signal receives contributions from final states across a range of hadronic mass, including hadronic systems with mass above that of the $K^*(892)$.

The branching fraction $\mathcal{B}$ for the signal is calculated from

$$\mathcal{B} = \frac{N_{sig}}{2N_{B\overline{B}}\,\epsilon}, \tag{2}$$

where $N_{B\overline{B}} = (88.9 \pm 1.0) \times 10^6$ is the number of $B\overline{B}$ pairs produced in 81.9 fb^{-1} and ϵ is the signal efficiency. The fitted signal yield N_{sig} contains a contribution from misreconstructed $B \to X_s\, \ell^+\ell^-$ decays (cross-feed events) of 1.8 ± 1.8 events in the electron channel and 0.9 ± 0.9 events in the muon channel. The central values are derived from fits to data in which the nominal fit function is changed to include a cross-feed PDF whose shape and normalization with respect to that for the correctly

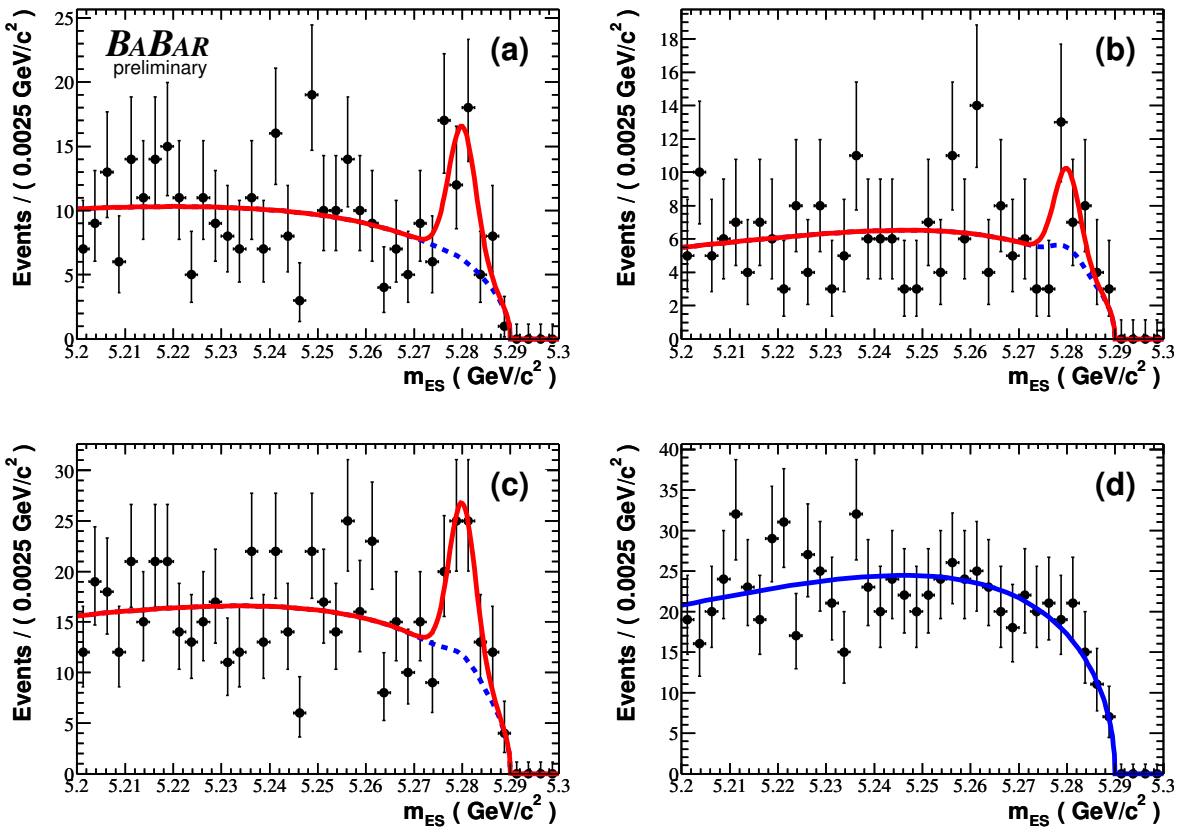

Figure 2: Distributions of m_{ES} for selected (a) $B \to X_s\, e^+e^-$, (b) $B \to X_s\, \mu^+\mu^-$, (c) $B \to X_s\, \ell^+\ell^-$ ($\ell = e, \mu$), and (d) $B \to X_s\, e^\pm\mu^\mp$ candidates. The solid lines represent the result of the fits and the dashed lines represent the background component under the signal peaks.

reconstructed $B \to X_s\, \ell^+\ell^-$ decays are taken from the simulation. The corresponding uncertainties are estimated from Monte Carlo studies using a large number of data-sized experiments. The signal efficiency ϵ is adjusted to reflect the contribution from cross-feed events.

7 Systematic uncertainties

Systematic uncertainties are of two different types: those that affect the extraction of the number of signal decays and those that affect the calculation of the branching fraction. The systematic uncertainties are summarized in Table 2.

Uncertainties affecting the extraction of the signal yield are evaluated by varying the signal Gaussian parameters (mean and width) and the signal shape (using asymmetric signal shapes) within the constraints allowed by the charmonium veto data. The small amount of peaking background from $B \to J/\psi\, X$ and $B \to \psi(2S)\, X$ decays is varied according to the estimated number of such decays: 0.6 ± 0.3 and 0.3 ± 0.2 in the electron and muon channels, respectively. The peaking background in the muon channel due to $B \to X_s\, \pi^+\pi^-$ decays is varied according to the estimated number of such events: 2.4 ± 0.8, where the uncertainty is dominated by the uncertainty in the

Table 1: Results of the fit to data: signal yield, charmonium and hadronic peaking backgrounds (fixed in the fit), combinatorial background yield, and statistical significance.

Sample	N_{sig}	N_{c-peak}	N_{h-peak}	N_{comb}	Signif.
$X_s\ e^+e^-$	29.0 ± 8.3	0.6	0.0	319.4 ± 18.9	4.0
$X_s\ \mu^+\mu^-$	12.4 ± 6.2	0.3	2.4	207.0 ± 15.2	2.2
$X_s\ \ell^+\ell^-$	41.4 ± 10.3	0.9	2.4	526.4 ± 24.3	4.6

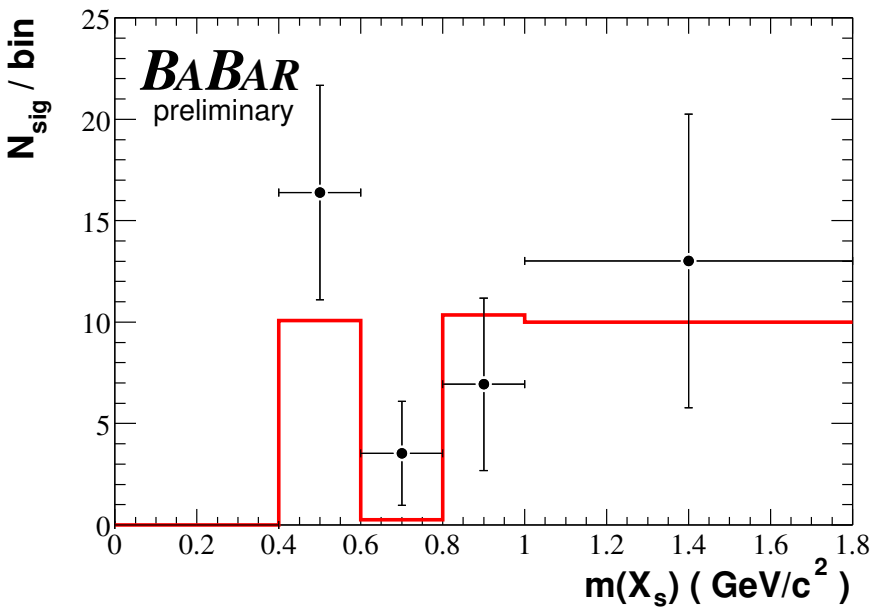

Figure 3: Distribution of number of signal events as a function of hadronic mass for electron and muon channels combined for data (points) and Monte Carlo signal (histogram). The vertical error bars represent statistical uncertainties only.

π to μ misidentification rates determined from control samples in the data. The shape of this background is also varied according to the data sample selected without lepton identification. The largest variations in the signal yield are observed for changes in the signal shape and in the amount of peaking background.

Uncertainties affecting the signal efficiency originate from the detector modeling, from the simulation of signal decays, and from the estimate of the number of B mesons in the sample. By far the dominant component is that due to the simulation of signal decays, discussed in detail below.

The detector modeling uncertainty is sensitive to the following uncertainties determined from the data: the uncertainty in the tracking efficiency of 1.3% per track (2.0% per charged pion); the uncertainty in the charged-particle identification efficiency of 0.7% per electron, 1.6% per muon, 1.0% per kaon and 2.0% per pion; and the uncertainty in the reconstruction efficiency of 10% per

K_S^0 and 5% per π^0. The efficiency of the likelihood ratio cut to suppress combinatorial background is checked with the charmonium-veto sample and the level of discrepancy with the simulation is taken as the corresponding uncertainty. The fraction of signal cross-feed included in the signal Gaussian is studied with a parameterized Monte Carlo simulation technique and the uncertainty is set to correspond to the R.M.S. obtained for a large number of data-sized experiments (the uncertainty amounts to a variation of $\pm 100\%$ of the number of signal cross-feed events included in the Gaussian).

The dominant source of uncertainty arises from modeling signal decays. Parameters of the Fermi motion model are varied in accordance with measurements of hadronic moments in semileptonic B decays [17] and the photon spectrum in inclusive $B \to X_s\,\gamma$ decays [18]. The fraction of exclusive $B \to K\ell^+\ell^-$ and $B \to K^*\ell^+\ell^-$ decays is varied according to theoretical uncertainties [1] and the corresponding systematic uncertainties are added linearly (i.e., we assume the uncertainties in the branching fraction for these two modes are fully correlated). The transition point in $m(X_s)$ between pure $K^*\ell^+\ell^-$ and nonresonant $X_s\,\ell^+\ell^-$ final states is varied by ± 0.1 GeV/c^2.

The nonresonant Monte Carlo event generator relies on JETSET to fragment and hadronize the system consisting of a final state s quark and a spectator quark from the B meson. Since the signal efficiencies depend strongly on the particle content of the final state, uncertainties in the number of charged and neutral pions and in the number of charged and neutral kaons translate into a significant uncertainty in the signal efficiency (for $m(X_s) > 1.1$ GeV/c^2).

The ratio between the generator yield for decay modes containing a K_S^0 and that for modes containing a charged kaon is varied according to 0.50 ± 0.05, to allow for isospin violation in the decay chain. The ratio between the generator yield for decay modes containing one π^0 and that for modes containing none is varied according to 1.0 ± 0.5. The ratio between the generator yield for decay modes into two-body hadronic systems and that into three-body hadronic systems is varied according to 0.5 ± 0.3. Uncertainties in the last two ratios are set by the level of discrepancy between data and Monte Carlo as measured in the *BABAR* semi-inclusive $B \to X_s\,\gamma$ analysis [19]. (Both $B \to X_s\,\gamma$ and present analyses use the same hadronization model.)

The ten modes selected in this analysis only capture about 50% of the full set of final states. Approximately half of the missing modes is due to final states with a K_L^0 meson and their contribution can be determined from the K_S^0 modes. However, we need to account for the uncertainty in the fraction of modes with too many pions or kaons (two extra kaons may be produced via $s\bar{s}$ popping), as well as for modes with photons that do not originate from π^0 decays but rather from η, η', ω, etc. For final states with $m(X_s) > 1.1$ GeV/c^2, we vary these different fractions by $\pm 50\%$.

Including systematic uncertainties, the measured branching fractions for $m(\ell^+\ell^-) > 0.2$ GeV/c^2 are

$$\mathcal{B}(B \to X_s\,e^+e^-) = \left(6.6 \pm 1.9^{+1.9}_{-1.6}\right) \times 10^{-6}, \quad (3)$$

$$\mathcal{B}(B \to X_s\,\mu^+\mu^-) = \left(5.7 \pm 2.8^{+1.7}_{-1.4}\right) \times 10^{-6}, \quad (4)$$

$$\mathcal{B}(B \to X_s\,\ell^+\ell^-) = \left(6.3 \pm 1.6^{+1.8}_{-1.5}\right) \times 10^{-6}, \quad (5)$$

where the first error is statistical and the second error is systematic. The combined $B \to X_s\,\ell^+\ell^-$ branching fraction is the weighted average of the branching fractions for the electron and muon channels, where we assume the individual branching fractions to be equal for $m(\ell^+\ell^-) > 0.2$ GeV/c^2. Table 3 summarizes the results of the analysis and lists both the statistical and systematic errors in the signal yields, the signal efficiencies and the branching fractions.

Table 2: Summary of fractional systematic uncertainties (in %). The uncertainties in extracting the signal are presented first and those related to the signal efficiency and $B\overline{B}$ counting are presented second.

Source	$X_s\, e^+e^-$	$X_s\, \mu^+\mu^-$
Signal shape	± 4.3	± 2.5
Peaking background	± 1.0	± 5.8
Signal yield total	± 4.4	± 6.3
Tracking efficiency	± 5.0	± 4.8
Lepton identification efficiency	± 1.3	± 3.2
Kaon identification efficiency	± 0.8	± 0.8
$\pi^\pm$ identification efficiency	± 1.5	± 1.3
K_S^0 efficiency	± 2.2	± 1.9
π^0 efficiency	± 0.8	± 0.5
LR cut efficiency	± 3.7	± 3.3
Cross-feed efficiency	± 6.7	± 7.4
Detector model subtotal	± 9.7	± 10.2
Fermi motion model	$^{+10.2}_{-4.0}$	$^{+10.8}_{-3.6}$
$\mathcal{B}(B \to K\ell^+\ell^-)$	± 9.6	± 12.6
$\mathcal{B}(B \to K^*\ell^+\ell^-)$	± 6.2	± 6.8
K^*–X_s transition	± 3.3	± 4.1
Hadronization	± 11.1	± 7.5
Missing modes	± 10.6	± 8.9
Signal model subtotal	$^{+24.5}_{-22.6}$	$^{+25.4}_{-23.3}$
Monte Carlo statistics	± 2.5	± 3.0
$B\overline{B}$ counting	± 1.1	± 1.1
Efficiency and $N_{B\overline{B}}$ total	$^{+26.5}_{-24.8}$	$^{+27.6}_{-25.6}$

8 Summary

Using a sample of 88.9×10^6 $\Upsilon(4S) \to B\overline{B}$ events, we measure the branching fraction for the rare decay $B \to X_s\, \ell^+\ell^-$, where $\ell = e$ or μ, with a sum over ten different hadronic states (with up to two pions). For $m(\ell^+\ell^-) > 0.2$ GeV/c^2, we observe a signal of $41 \pm 10(stat) \pm 2(syst)$ events and obtain a branching fraction of

$$\mathcal{B}(B \to X_s\, \ell^+\ell^-) = \Big(6.3 \pm 1.6(stat)^{+1.8}_{-1.5}(syst)\Big) \times 10^{-6}, \tag{6}$$

with a statistical significance of $4.6\,\sigma$. This preliminary measurement agrees well with the recent prediction by Ali *et al.* [1] and the measurement performed by the Belle Collaboration, $\mathcal{B}(B \to X_s\, \ell^+\ell^-) = (6.1 \pm 1.4(stat) \pm^{1.4}_{1.1} (syst)) \times 10^{-6}$ for $m(\ell^+\ell^-) > 0.2$ GeV/c^2 [7].

Table 3: Summary of results: signal yield, statistical significance, efficiency and branching fraction. In the case of the signal yield and the branching fraction, the first error is statistical and the second error is systematic. In the case of the signal efficiency, the first error corresponds to uncertainties in detector modeling, $B\overline{B}$ counting, and Monte Carlo statistics, whereas the second error corresponds to the uncertainties in the signal model.

Sample	N_{sig}	Signif.	ϵ (%)	$\mathcal{B}$ ($\times 10^{-6}$)
$X_s\, e^+e^-$	$29.0 \pm 8.3 \pm 1.3$	4.0	$2.46 \pm 0.25^{+0.60}_{-0.56}$	$6.6 \pm 1.9^{+1.9}_{-1.6}$
$X_s\, \mu^+\mu^-$	$12.4 \pm 6.2 \pm 0.8$	2.2	$1.23 \pm 0.13^{+0.31}_{-0.29}$	$5.7 \pm 2.8^{+1.7}_{-1.4}$
$X_s\, \ell^+\ell^-$	$41.4 \pm 10.3 \pm 1.5$	4.6	—	$6.3 \pm 1.6^{+1.8}_{-1.5}$

Acknowledgments

The authors wish to thank Gudrun Hiller for her help. We have also benefitted from discussions with Tobias Hurth.

We are grateful for the extraordinary contributions of our PEP-II colleagues in achieving the excellent luminosity and machine conditions that have made this work possible. The success of this project also relies critically on the expertise and dedication of the computing organizations that support *BABAR*. The collaborating institutions wish to thank SLAC for its support and the kind hospitality extended to them. This work is supported by the US Department of Energy and National Science Foundation, the Natural Sciences and Engineering Research Council (Canada), Institute of High Energy Physics (China), the Commissariat à l'Energie Atomique and Institut National de Physique Nucléaire et de Physique des Particules (France), the Bundesministerium für Bildung und Forschung and Deutsche Forschungsgemeinschaft (Germany), the Istituto Nazionale di Fisica Nucleare (Italy), the Foundation for Fundamental Research on Matter (The Netherlands), the Research Council of Norway, the Ministry of Science and Technology of the Russian Federation, and the Particle Physics and Astronomy Research Council (United Kingdom). Individuals have received support from the A. P. Sloan Foundation, the Research Corporation, and the Alexander von Humboldt Foundation.

References

[1] A. Ali, E. Lunghi, C. Greub, and G. Hiller, Phys. Rev. D **66**, 034002 (2002).

[2] T. Hurth, `hep-ph/0212304`, SLAC–PUB–9604 (2003).

[3] A. Ali, `hep-ph/0210183`, CERN–TH/2002-284 (2002).

[4] K. Abe *et al.* (Belle Collaboration), Phys. Rev. Lett. **88**, 021801 (2002).

[5] B. Aubert *et al.* (*BABAR* Collaboration), `hep-ex/0207082`, SLAC–PUB–9323 (2002).

[6] A. Ryd, talk presented at the International Europhysics Conference on High Energy Physics EPS, 17–23 July 2003, Aachen, Germany.

[7] J. Kaneko *et al.* (Belle Collaboration), Phys. Rev. Lett. **90**, 021801 (2003).

[8] The technique based on summing exclusive modes was introduced in the context of inclusive $B \to X_s\,\gamma$ decays; see M. S. Alam *et al.* (CLEO Collaboration), Phys. Rev. Lett. **74**, 2885 (1995).

[9] B. Aubert *et al.* (*BABAR* Collaboration), Nucl. Instrum. Methods **A479**, 1 (2002).

[10] B. Aubert *et al.* (*BABAR* Collaboration), Phys. Rev. D **66**, 032003 (2002).

[11] A. Ali, P. Ball, L.T. Handoki, and G. Hiller, Phys. Rev. D **61**, 074024 (2000).

[12] F. Krüger and L.M. Sehgal, Phys. Lett. B **380**, 199 (1996).

[13] A. Ali and E. Pietarinen, Nucl. Phys. B **154**, 519 (1979); G. Altarelli *et al.*, Nucl. Phys. B **208**, 365 (1982).

[14] T. Sjöstrand, Computer Physics Commun. 82, 74 (1994).

[15] G.C. Fox and S. Wolfram, Phys. Rev. Lett. **41**, 1581 (1978).

[16] H. Albrecht *et al.* (ARGUS Collaboration), Phys. Lett. B **192**, 245 (1987).

[17] D. Cronin-Hennessy *et al.* (CLEO Collaboration), Phys. Rev. Lett. **87**, 251808 (2001).

[18] S. Chen *et al.* (CLEO Collaboration), Phys. Rev. Lett. **87**, 251807 (2001).

[19] B. Aubert *et al.* (*BABAR* Collaboration), `hep-ex/0207074`, SLAC–PUB–9308 (2002).